PERFORMANCE OF GEOGRID REINFORCED SOIL BARRIERS OF LANDFILL COVERS: A CENTRIFUGE STUDY

S. Rajesh
Assistant Professor, Department of Civil Engineering, Indian Institute of Technology Kanpur, Kanpur, India;
Tel: +91 542 259 6054; Fax: +91 542 259 7395; Email: hsrajesh@iitk.ac.in (former Research Scholar,
Department of Civil Engineering, Indian Institute of Technology Bombay, Mumbai, India).

ABSTRACT

The objective of this paper is to evaluate the deformation behavior of geogrid reinforced soil barriers of landfill covers using centrifuge model studies. Centrifuge model tests were performed at 40g on soil barriers reinforced with and without scale-down model geogrid subjected to continuous differential settlements using a 4.5 m radius beam centrifuge having a capacity of 2500 g-kN available at IIT Bombay. Differential settlements were induced using a motor-based differential settlement simulator designed for a high gravity environment. Strain gauge based instrumented scale – down model geogrids were used to estimate the actual mobilized tensile load of geogrids at various levels of distortion. Centrifuge model test results reveal that a 1.2 m thick unreinforced soil barrier subjected to an overburden pressure equivalent to that of a cover system experienced cracks extending up to full thickness of the soil barrier and lost its integrity at low distortion levels. A substantial reduction in the magnitude of crack width and depth were noticed when the soil barrier was reinforced with low strength geogrid. In the case of a soil barrier reinforced with a high strength geogrid, the soil barrier was observed to be free from cracking even after subjecting to a distortion level of 0.125. The reason for the significant improvement in the performance of geogrid reinforced soil barrier is attributed to the soil-geogrid interaction and mobilization of tensile load of geogrid layer at the onset of differential settlements. The mobilization of tensile load of geogrid was found to increase with an increase in the geogrid strength, which in-turn, helps in restraining soil crack potential even after subjecting to large distortions.

Keywords: Geogrid, soil barrier, centrifuge modeling, differential settlement

INTRODUCTION

Waste disposal through engineered landfills is one of the most popular waste treatment systems that are currently in practice in most countries. Engineered landfills comprise various layers of soil and geosynthetics, based on the type of waste, thickness of waste to be contained, desirable period of post-closure monitoring, geological and geotechnical constraints, financial constraints etc. However, every landfill should have an impervious layer in all lining systems (top, bottom and side) intended to control infiltration of liquid and gas into or from the waste. Clay-rich soils can be considered as an effective and economical barrier material provided it has a coefficient of permeability of 1 x 10^{-9} m/s or less. However, a soil barrier is susceptible to cracking due to moisture fluctuations (desiccation cracks) and differential settlements (mainly due to readjustments and decomposition of the contained wastes). Excessive differential settlements can result in the development of tension cracks on soils (cover soil / soil barrier), tensile or shear failures in barrier materials (soil barrier / geomembranes), and the formation of sinkhole-type localised depressions in the cover which can result in ponding of water. This made several researchers to work towards the development of crack free barrier at the onset of differential settlements.

Deformation behavior of soil barriers under wide range of distortion levels can be studied using actual field settlement monitoring, full-scale testing, reduced–scale testing (normal gravity and accelerated gravity) and / or numerical solutions (Lee and Shen 1969, Jessberger and Stone 1991, Viswanadham and Rajesh 2009, Rajesh and Viswanadham 2012b). The distortion level a/l is defined as the ratio of central settlement a at any stage of deformation to the influence length l within which differential settlements are induced. Many researchers adopted centrifuge modeling technique to understand the deformation behavior of soil barriers mainly because of its merit in simulating the identical stress-strain behavior as prototype (Schofield 1980). Several researchers carried out centrifuge tests on clay based hydraulic barrier subjected to differential settlements and found that the soil barrier having thickness ranging from 0.6 m to 1.2 m tends to experience severe cracking at low distortion levels (Jessberger and Stone 1991, Viswanadham and Mahesh 2002). The cracking of the soil barrier was primarily due to the low tensile

strength of the soil barrier material. It was also reported that attenuation of cracking in soil barriers was noticed with an increase in the thickness of the soil barrier, consistency of the soil barrier material and overburden pressure. Various researchers tried different methods for improving the deformation behavior of the soil barrier against differential settlements like mixing discrete fibers with soil barrier, or placing geogrid within the soil barrier (Viswanadham et al. 2011, Rajesh and Viswanadham, 2012a). In the present study, an attempt has been made to study the influence of geogrid reinforcement on the deformation behavior of the soil barrier under various ranges of distortion level by introducing strain gauge based instrumented scale-down model geogrid within the soil barrier using centrifuge model testing facility available at IIT Bombay.

MDSS SYSTEM

The differential settlements are simulated in a centrifuge using a custom designed and developed Motor based Differential Settlement Simulator (MDSS). MDSS system works on a simple principle where the rotational movement of the motor is converted to translation movement of the central platform. Figure 1 shows the schematic view of the MDSS system. The central gear is connected to the 42 mm outer diameter screw jack with 4.5 mm pitch and in-turn connected to central platform. A false base containing a pair of 100 mm hinged flaps is placed on the central platform. When the motor rotates with the help of the thyristor based motor controller, gear train rotates, which in-turn make the screw jack to rotate. Since the screw jack is connected to the central platform, as the screw jack rotates, the central platform (restrained to rotation) lowers with a suitable settlement rate and rotates the hinged flap and induces a discontinuity of slope at the base of overlying soil (Rajesh and Viswanadham, 2010).

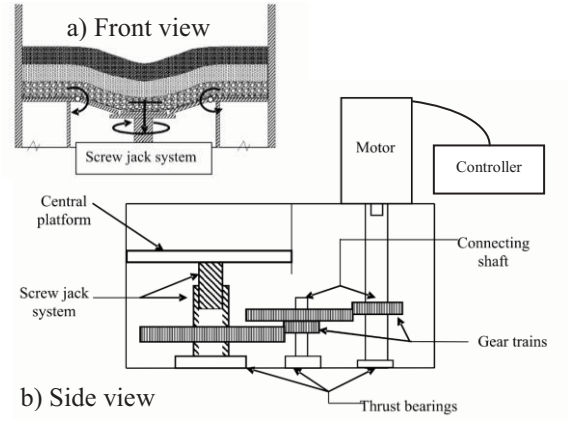

Fig. 1 Schematic representation of MDSS system.

MODEL MATERIALS AND TESTING PROCEDURE

Model Materials

Various mix ratios of kaolin clay and sand were tried to choose the model soil barrier in such a way that it represents the properties of soil barrier material used in the construction of landfill covers. As the properties of mixture of commercially available kaolin clay and locally available poorly graded sand in proportion of 80:20 (by dry weight) are within the range of compacted soil barrier material characteristics used in actual practice in many landfills in the USA, it was selected as a model soil barrier (Benson et al. 1999). It has liquid a limit of 38%, a plastic limit of 16%, a coefficient of permeability of 0.4×10^{-9} m/s. Since, most of the landfill barrier (cover) layers present in municipal and low-level radioactive waste disposal system are compacted at the wet side of optimum, it is decided to work with OMC + 5% water content. The model soil barrier was moist-compacted at a moulding water content of OMC + 5% with the corresponding dry unit weight of 14.2 kN/m^3 using standard Proctor compaction test results.

Several investigators like Springman et al. (1992), and Viswanadham & König (2004) attempted to model the geogrid reinforcement for understanding the behavior of reinforced soil structures at normal gravity conditions and/or at accelerated gravity conditions. Centrifuge scaling factors relevant to modeling of geogrid reinforcement has been described elsewhere extensively by Viswanadham & König (2004). In the present study, two model scale-down geogrids namely GR2 and GR9 were selected such that they represent properties of the commercially available geogrids having high and low tensile load-strain characteristics. The average wide-width tensile load of model geogrids GR2 and GR9 corresponding to 5% strain are 4.51 kN/m and 0.287 kN/m respectively (in model dimensions); at 40 gravities, is approximately 180 kN/m and 11 kN/m respectively. In addition, it was ensured that the percentage open area of model geogrids is representing the percentage open area range of commercially available geogrids. The aperture sizes of both the model geogrids is 3.5 mm x 3.5 mm (in model dimensions) with the percentage opening area which depends on the rib dimensions was found to be 68% and 92% for model geogrids GR2 and GR9 respectively.

Strain Gauge Based Instrumentation for Scale-Down Model Geogrids

In the present study, an attempt has been made to measure the mobilized tensile load of the geogrid

layer at various ranges of distortion levels using calibrated strain gauge based instrumented scale-down geogrids. Strain gauges of 0.6 mm in length, 0.8 mm in width and a base of 5.3 mm x 1 mm with a nominal resistance of 120Ω, gauge length of 0.6 mm, gauge factor of 2.24 and strain limit of 3% were used. As the average width of ribs of scale-down model geogrids (ranging from 0.5 mm to 1.5 mm) are very small, pasting of strain gauges on to ribs will not be possible and even if it is done, the response could be highly localized. Hence, few researchers preferred to fill geogrid opening sizes using epoxy type backing material with strain gauges pasted on to a hardened backing material (Springman et al. 1992, Viswanadham and König, 2004). In this study, a 25 mm x 25 mm square portion in the centre of the selected geogrid specimen was filled with 2 mm thick rubber-based backing material. This backing material was chosen due to its tough, flexible, film-forming characteristics with good resistance to heat and ageing. Strain gauges were oriented in such a way that they can only measure the tensile strain. In order to avoid bending effect, two active strain gauges were pasted on both sides of the backing material. Two dummy strain gauges for each channel were pasted on to a 6 mm thick Perspex sheet coated with a rubber-based backing material, identical to the one used on model geogrids, to facilitate temperature compensation. A water-proofing sealant was applied on the strain gauges and the soldered ends of lead wires to avoid any contact of water with the electrical connections.

A custom designed and developed load-based calibration test setup was used to calibrate instrumented model geogrids by measuring the change in resistance, which in-turn can be used to determine mobilized tensile load of geogrid under various magnitude of loads. The obtained calibration factors were used for determining the mobilized tensile load of the geogrid embedded within the soil, while inducing differential settlements in a centrifuge. The detailed explanation covering the selection of backing material, layout of strain gauges, calibration procedure and the calibration charts can be obtained from Rajesh and Viswanadham (2012a).

Test Program

In the present study, the influence of geogrid reinforcement on the deformation behavior of clay-based landfill covers at the onset of differential settlements was studied using three centrifuge tests (URSB, GRSB1 and GRSB2) at 40 gravities. The thickness of the soil barrier adopted in this study is 1.2 m. Since the thickness of the cover soil along with water drainage layer placed above the soil barrier in the cover system (of about 1 m to 1.5 m thick) can generate an overburden pressure of 25 kPa, an overburden pressure of 25 kPa was created above the soil barrier at 40 gravities. The selected model geogrid was placed at 1/4th of the thickness of the soil barrier from top surface of the soil barrier ($d_g = 0.25d$). The position of the geogrid was chosen because of its effectiveness when compared to other positions (Kuo & Hsu 2003). The performance of geogrid reinforced soil barriers (GRSBs) was assessed by varying geogrid type while keeping gravity level, settlement rate, moist-compacted conditions of the model soil barrier material, thickness of the soil barrier, overburden pressure and position of the geogrid as constant.

Model Preparation

A container having internal dimensions of 720 mm x 450 mm x 440 mm was used in the present study. Figure 2 show the front view of the test setup (after being subjected to a distortion level of 0.125) along with soil layers and sensors used in the present study. Permanent markers are placed in the pre-determined locations so that image analysis can be performed. The MDSS system is placed inside the container and the horizontal level surface was maintained and was verified using a spirit level. To avoid the stress concentration near the hinges, sacrificial layer of 30 mm thick coarse sand layer was provided, followed by 30 mm thick fine sand layer and in turn followed by the thick non-woven geotextile pieces as shown in Figure 2. The kaolin clay-sand mixture was moist-compacted with OMC+5% and corresponding dry unit weight (14.2 kN/m^3). In the case of the geogrid reinforced soil barrier, the model geogrid was placed without any undulations and pre-stressing at d_g (i.e., 0.25d) from the top surface of the clay barrier. Upon completion of the soil barrier layer, a seating pressure of 5 kPa (static load of 1.4 kN) was applied uniformly for about 5 hour on soil barrier in order to achieve proper contact between the soil and geogrid layer.

Plastic markers were stuck using an instant adhesive along the cross-section at every 20 mm centre to centre distance to the model geogrid layer to measure its deformation profile during various stages of the centrifuge test. Five numbers of Pore Pressure Transducer (PPTs) (Type PDCR81 manufactured by Druck Limited, United Kingdom) were placed above the soil barrier to monitor the water level and to determine the water breakthrough. The overburden pressure of 25 kPa was placed above the model soil barrier layer (created using 27 mm thick sand layer and 10 mm high inundated water). In order to avoid leakage of water between the sides of the container and the soil barrier, water tight seal made up of a thick bentonite paste was applied all along the sides of the soil barrier. Side bunds were provided along the breadth of the

container to prevent leakage of water and to provide anchorage to the geogrid layer (Fig. 2).

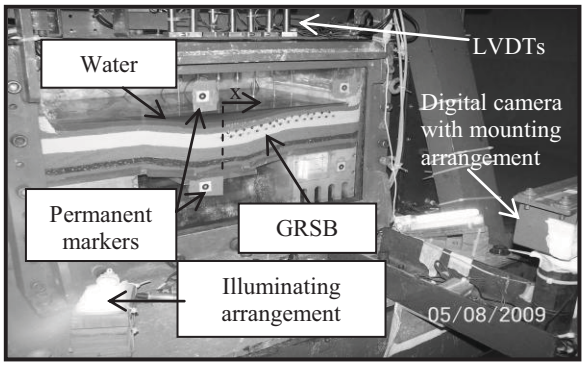

Fig. 2 Front view of model test package after inducing distortion level of 0.125

A linear variable differential transformer (LVDT) was attached to the central platform of MDSS system so as to measure induced central settlement *a* and monitor the settlement rate and six LVDT's was placed on the surface of the sand layer to measure the deformation profile. A digital photo camera was placed along with the model, on the front side of the model; Charge Coupled Device (CCD) video camera was mounted on the top of the model to monitor the depletion of water level during centrifuge test. The motor of the MDSS system was switched on at 40g and desired speed of the motor was set with the help of the controller to achieve a settlement rate of 1 mm/min. At the various stages of central settlements, photographs were taken through image acquiring software and were later used for image analysis to compute deformation profiles using front camera.

ANALYSIS AND INTERPRETATION

Table 1 summarizes the results of the centrifuge tests carried out to study the deformation behavior of the soil barrier with and without the inclusion of geogrid reinforcement.

Deformation Pattern

The photographs captured at various stages of central settlement through a digital photo camera were used to determine the displacement of the discrete markers with respect to a rectangular grid of markers permanently fixed onto the inner side of the Perspex sheet. The coordinates of each discrete marker at various stages of central settlements were determined using digitization of the discrete markers using GRAM++ (2004). The measured coordinates of markers fixed in the soil and geogrid are approximated with an exponential equation of the normal distribution to get the deformation profile of soil and geogrid layer at various stages of central settlement. Figure 3 shows the displacement profiles of the top surface of the 1.2 m thick soil barrier with and without geogrid for various stages of central settlements. It can be observed that both the un-reinforced soil barrier [Model: URSB] and geogrid reinforced soil barrier [Model: GRSB2] experienced almost identical displacement profiles at the various stages of central settlements; however, the model GRSB2 was found to deform relatively more when compared to the URSB

Table 1 Summary of test results

Parameters	URSB	GRSB1	GRSB2
Type of soil barrier	Unreinforced soil barrier	GRSB (GR9)	GRSB (GR2)
d (mm)	1200 (30)	1200 (30)	1200 (30)
σ_o (kPa)	25	25	25
ε_{max} (%)	3.81	4.01	3.76
d_c (mm)	1200 (30)	680 (17)	Negligible
$(a/l)_{lim}$	0.069	0.108	0.125
Cracking pattern	Full depth -narrow crack	Fine crack extending to partial depth	Tiny surface cracks

d- thickness of the soil barrier; d_c – depth of crack measured from the top surface of the soil barrier; σ_o – overburden pressure; ε_{max}- maximum tensile strain at the zone of maximum curvature; $(a/l)_{lim}$- limiting distortion level; Values in model dimensions are given within the parenthesis.

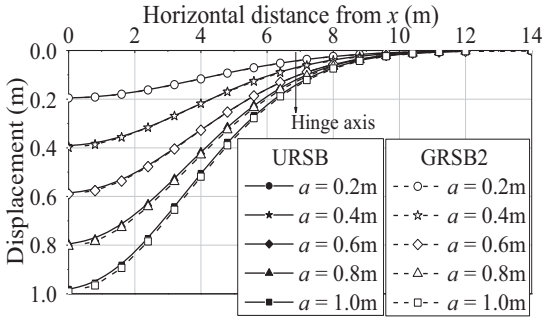

Fig. 3 Displacement profiles measured at the top surface of the soil barrier with and without geogrid reinforcement for various central settlements [Models: URSB and GRSB2]

Strain Distribution Pattern

Displacement profiles obtained at various stages of central settlement were used to determine the strain along the top surface of the soil barrier. If $w_s(x)$ is the function of displacement profile of the top surface of the soil barrier and $w_s'(x)$ and $w_s''(x)$ are the first and second derivatives of $w_s(x)$, then the soil strain ε_s can be computed using combined bending and elongation method (Lee and Shen, 1969) as follows:

$$\varepsilon_s = \varepsilon_{ls} \pm R_{of}\kappa_s d \quad (1)$$

Similarly the geogrid strain (ε_g) can be determined as follows:

$$\varepsilon_g = \varepsilon_{lg} \pm (R_{of} - d_g)\kappa_g d \quad (2)$$

Soil strain at the geogrid interface ε_{sg} can be determined from ε_s, assuming linear variation of strain across the thickness of the soil barrier:

$$\varepsilon_{sg} = \frac{(R_{of} - d_g)}{R_{of}}\varepsilon_s \quad (3)$$

where, $\varepsilon_l = \sqrt{1+[w'(x)]^2} - 1$ (4)

and R_{of} = neutral axis factor (=0.67); κ = curvature at any horizontal distance = $w''(x)$; $w(x)$ is the equation of the displacement profile, subscript s and g denotes soil and geogrid respectively.

The strain distribution of the 1.2 m thick un-reinforced soil barrier (URSB) subjected to an overburden pressure of 25 kPa at various stages of central settlement is shown in Fig. 4a [Model: URSB]. It can be observed that as the central settlement increases, both the tensile and compressive strains along the top surface of the soil barrier also increases at the zone of tension and compression zone respectively. Figure 4b shows the variation of strains in geogrid and the soil along the soil-geogrid interface with the horizontal distance from the centre of the soil barrier, for the soil barrier reinforced with an instrumented geogrid GR2 [Model: GRSB2]. At lower central settlements, the geogrid strain distribution and the soil strain distribution at the geogrid interface are almost identical. However, for higher central settlements, geogrid strains are relatively higher when compared to the soil strain at the geogrid interface. The participation of geogrid in the load transfer mechanism can be understood from the higher geogrid strain. Moreover, variation between geogrid and soil strains at the interface, all along the length of the barrier increases with an increase in the central settlement.

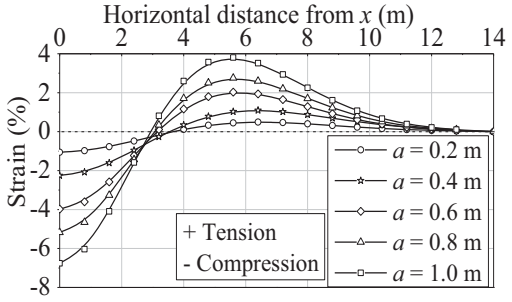

a) Soil strain (ε_s) distribution [Model: URSB]

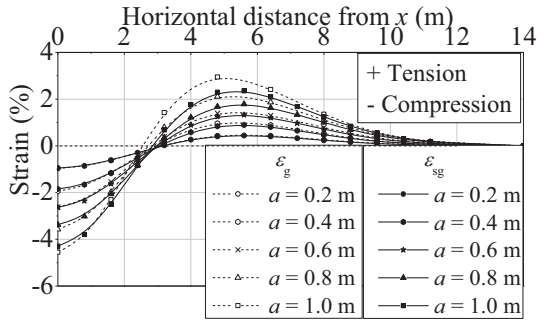

b) Strains in soil and geogrid along the soil-geogrid interface (ε_{sg}, ε_g) [Model: GRSB2]

Fig. 4 Variation of strain distribution along the horizontal distance from the center of the soil barrier [Models: URSB and GRSB2]

The variation of maximum tensile soil strain along the top surface of various soil barriers with settlement ratio a/a_{max} and distortion level a/l is plotted as shown in Figure 5. It can be observed that for all soil barriers, as the distortion level increases, the maximum tensile strain also increases and the variation is almost linear even after crack initiation. The strain at crack initiation of the URSB was found to less than the soil barrier reinforced with low strength model geogrid [Model: GRSB1].

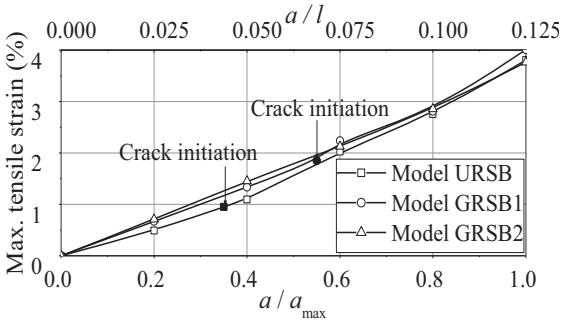

Fig. 5 Variation of maximum tensile strain at the zone of maximum curvature with a/a_{max} and a/l for all centrifuge tests.

Water Breakthrough Pattern

The performance of the soil barrier as an effective hydraulic barrier can be best illustrated from the flow of water through the soil barrier. The severity of the water breakthrough and the integrity of the tested barrier at the onset of differential settlements were analyzed in this study, with the help of known volume of water kept above the top surface of the soil barrier. Measurements from the miniature pore pressure transducers (PPTs) placed on the soil barrier at predefined locations were used to determine the pore water pressure at various stages of central settlements. From the pore water pressure measurements, the height of water present above every PPTs (i.e., water profile) can be determined at various stages of central settlement. The volume of water can be determined as the product of the width of the soil barrier and area under measured water profile (i.e., numerical integration). The change in the volume of water at any settlement stage can be obtained from the numerical difference between the initial volume of water v_o to the volume of water at the required settlement stage v_a. The initial volume of water computed by numerical integration was crosschecked with the actual measured value of water placed above the soil barrier. The reduction in volume of water is possible only due to the infiltration of the water either through pore spaces presents in the soil barrier or through the crack formation. Proper care has been taken while preparing all models to avoid the leakage of water other than infiltration, by providing side bunds and all round water sealing arrangement in the form of thick bentonite paste (refer to Figure 2). From post-test examinations of deformed soil barriers, it was confirmed that there was no side leakage for all models.

The infiltration ratio IFR can be determined from Eq. 5:

$$IFR = \frac{v_0 - v_a}{v_0} \quad (5)$$

The variation in the magnitude of infiltration ratio with the settlement ratio and distortion level for the 1.2 m thick soil barrier with and without geogrid reinforcement was plotted, as shown in Fig. 6. It can be noticed that a gentle variation in IFR occurs up to a certain distortion level followed by a steep variation (water breakthrough of the soil barrier). When the cracks extend sufficient width and depth, water has a tendency to flow through the barrier and IFR increases. The distortion level corresponding to the water breakthrough is termed as limiting distortion level $(a/l)_{lim}$. The limiting distortion level can be determined using a back tangent method. The limiting distortion level for the 1.2 m thick URSB was found to be 0.069 [Model: URSB]. When the soil barrier was reinforced with low strength geogrid (GR9), the limiting distortion level was increased to 0.108 [Model: GRSB1]. It can be noticed from Fig. 6 that when a high strength geogrid (GR2) was used, no significant variation in IFR values was observed, which implies that a negligible infiltration of water through the soil barrier [Model: GRSB2]. This model barrier has sustained a distortion level of 0.125, which is the maximum value that can be induced using the MDSS used in the present study. This indicates that sealing efficiency of a 1.2 m thick GRSB can be maintained during all stages of distortion level (maximum a/l of 0.125), if it is reinforced with a geogrid layer having tensile load-strain characteristics within the range of properties of GR2 and GR9. The strain corresponding to limiting distortion has increased from 1.75% to 3.78% when the soil barrier was reinforced with high strength model geogrid.

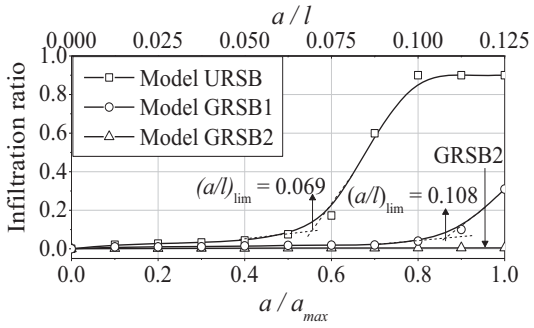

Fig. 6 Variation of infiltration ratio with a/a_{max} and a/l for all centrifuge tests

Cracking Pattern

The status of 1.2 m thick soil barrier with and without geogrid reinforcement after inducing central settlement of 1 m and distortion level of 0.125 is shown in Fig. 7. A clear distinct full-depth crack can be observed for the URSB. Partial penetration of crack with the average crack depth of 17 mm was noticed when the soil barrier was reinforced with a low strength geogrid [Model: GRSB1]. Interestingly, with the introduction of high strength geogrid (GR2) within the soil barrier, crack free soil barrier has been obtained even at a distortion level of 0.125, which clearly demonstrates the effectiveness of geogrid reinforcement. The partial penetration of crack was the reason for the steep rise in the value of infiltration ratio at higher distortion level. In addition, the reason behind the formation of partial penetration of fine cracks in GRSB could be due to inadequate mobilization of the required tensile load along the soil-geogrid interface at the onset of differential settlements.

a) Cross-sectional view (Model URSB)

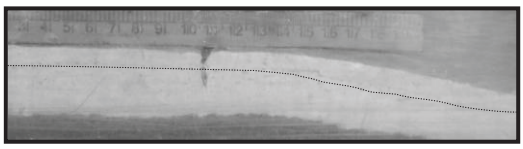

b) Cross-sectional view (Model GRSB1)

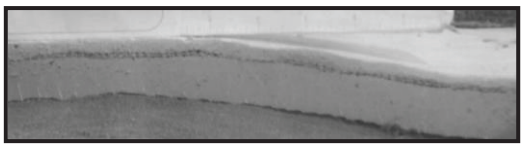

c) Cross-sectional view (Model GRSB2)

Fig. 7 Status of soil barriers with and without geogrid reinforcement at the end of centrifuge tests

Mobilized Tensile Load Distribution Pattern

The mobilization of the tensile load of the geogrid at various ranges of central settlement and distortion level can be obtained from instrumented geogrids. A distinct increase in the maximum mobilized tensile load at the zone of maximum curvature was observed with an increase in the central settlement and distortion level. Figure 8 presents the variation of maximum mobilized tensile load of the geogrid against settlement ratio and distortion level for the soil barrier with low strength geogrid (GR9) and high strength geogrid (GR2). At every stage of central settlement, high strength geogrid could mobilize higher tensile load when compared to low strength geogrid. For a central settlement of 0.4 m, the low strength model geogrid could generate a maximum tensile load of 16 kN/m when compared to 72 kN/m for a high strength geogrid. The maximum mobilized tensile load experienced by high strength geogrid at a central settlement of 1 m (a/l = 0.125) was found to be 120 kN/m [Model: GRSB2], as compared to 37 kN/m for low strength geogrid [Model: GRSB1]. In addition, for central settlements of a = 0.8 m and a = 1 m, the maximum mobilized tensile load of high strength geogrid was found to be almost constant, which indicates that the geogrid layer has generated the maximum possible mobilization of the tensile load. This shows the importance of selection of suitable geogrid type. From the earlier discussion, it can be noted that the soil barrier reinforced with geogrid GR2 was found to exhibit crack free behavior with negligible infiltration even at a central settlement of 1 m (a/l = 0.125; a/a_{max} = 1). This study demonstrates that when a 1.2 m thick soil barrier is reinforced with a geogrid having a tensile load of 120 kN/m (without adopting any safety factors), a crack free barrier can be ascertained even at a distortion level of 0.125.

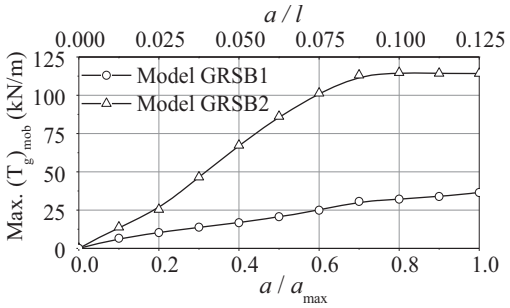

Fig. 8 Variation of maximum mobilized tensile load at the zone of maximum curvature with a/a_{max} and a/l

CONCLUSIONS

A series of centrifuge model tests were performed on 1.2 m thick soil barriers with and without the inclusion of an instrumented geogrid reinforcement layer to study the sealing efficiency of soil barriers and tensile load distribution under various distortion levels. Based on the analysis and interpretation of centrifuge test results, the following conclusions can be drawn:

- A 1.2 m thick un-reinforced soil barrier subjected to an overburden pressure equivalent to a landfill cover system was found to experience narrow cracks at the zone of maximum curvature, with the depth of cracks extending up to full-thickness of the soil barrier. A substantial reduction in the magnitude of crack width and depth were noticed when the soil barrier was reinforced with low strength geogrid. Interestingly with the inclusion of high strength geogrid within the soil barrier, crack free soil barrier was noticed even after inducing distortion level of 0.125.
- The limiting distortion level of URSB was found to be 0.069. With the inclusion of low strength geogrid within the soil barrier, limiting distortion level was increased to 0.108. When a high strength geogrid was reinforced within the soil barrier, soil barrier has sustained a distortion level of 0.125 without loss of integrity.
- The maximum mobilized tensile load of low strength model geogrid at a distortion level of 0.125 was found to be 37 kN/m. However, for identical conditions with high strength geogrid, it was observed to increase to 120 kN/m.

This study concludes that the performance of a GRSB was found to be many times superior to the respective URSB in terms of both restraining cracks and a substantial delay in water breakthrough. In addition, it is clearly demonstrated that when a soil barrier is reinforced with a suitable geogrid having adequate tensile load- strain characteristics, it can retain the integrity and maintain the desired sealing efficiency even at a higher distortion level.

ACKNOWLEDGEMENTS

Author would like to thank the Centrifuge team at the National Geotechnical Centrifuge Facility of Indian Institute of Technology Bombay, Powai, Mumbai-400076, India for their untiring support throughout the present study.

REFERENCES

Benson C.H. Daniel, D.E. and Boutwell, G.P. (1999). Field performance of compacted clay liners. Journal of Geotechnical and Geoenvironmental Engineering, ASCE 125(5): 391–403.

GRAM ++. 2004. http://www.csre.iitb.ac.in/ gram++/

Jessberger H.L. and Stone K.J.L. (1991). Subsidence effect on clay barriers. Geotechnique, 41(2): 185–194.

Kuo C.M. and Hsu T.R. (2003). Traffic induced reflective cracking on pavements with geogrid reinforced asphalt concrete overlay. Proc Annual Meeting of the Transportation Research Board (CD-ROM), Transportation Research Board, Washington, DC: 1–23.

Lee K.L. and Shen C.K. (1969). Horizontal movements related to subsidence. Journal of Soil Mechanics and Foundation division, ASCE. 94 (6): 139–166.

Rajesh S. and Viswanadham B.V.S. (2010). Development of a motor-based differential settlement simulator setup for a Geotechnical Centrifuge. Geotechnical Testing Journal, ASTM, 33(6): 507-513.

Rajesh S. and Viswanadham B.V.S. (2012a). Modelling and instrumentation of geogrid reinforced soil barriers of landfill covers. Journal of Geotechnical and Geoenvironmental Engineering, ASCE, 138(1): 26-37.

Rajesh S. and Viswanadham B.V.S. (2012b). Centrifuge and numerical study on the behavior of soil barriers under differential settlements. Journal of Hazardous, Toxic, and Radioactive Waste, ASCE. (doi:10.1061/(ASCE)HZ.2153-5515.0000129).

Schofield A.N. (1980). Cambridge geotechnical centrifuge operations. Geotechnique, 30(3): 227–268.

Springman S. Bolton M. Sharma J. and Balachandran S. (1992). Modeling and instrumentation of a geotextile in the geotechnical centrifuge. Proc International Symposium on Earth Reinforcement Practice, Fukuoka, Japan, Ochiai, H., Hayashi, S., Otani, J. (Eds.), A.A. Balkema, Rotterdam, 1: 167–172.

Viswanadham B.V.S. and Mahesh K.V. (2002). Modeling deformation behaviour of clay liners in a small centrifuge. Canadian Geotechnical Journal. 39(6): 1406-1418.

Viswanadham B.V.S. and König D. (2004). Studies on scaling and instrumentation of a geogrid. Geotextiles and Geomembranes. 22(5): 307-328.

Viswanadham B.V.S. and Rajesh S. (2009). Centrifuge model test on clay based engineered barriers subjected to differential settlement. Applied Clay Science. 42(3-4): 460-472.

Viswanadham B.V.S. Rajesh S. Divya P. V. and Gourc J.P. (2011). Influence of randomly distributed geofibers on the integrity of clay-based landfill covers: a centrifuge study. Geosynthetics International. 18(5): 255–27.